

# **PREDICTION OF THE BEHAVIOR OF LIME MORTAR REINFORCED WITH FIBERS BASED ON THEIR MICROMECHANICAL PARAMETERS**

*Michal Přinosil<sup>1</sup>, Petr Kabele<sup>2</sup>*

## **ABSTRACT**

For the purpose of restoration works a new fiber reinforced composite material with lime matrix is being developed. Fibers act as dispersed reinforcement, which, after matrix cracking, ensures that the material retains macroscopic integrity and makes it possible to limit the cracks width. The behavior of individual cracks in fiber composite can be controlled by its composition and by the micromechanical parameters of fibers, matrix and the fiber-matrix interface, which we utilize to optimize the material design. To this end, we have chosen several types of fibers and their micromechanical parameters and the parameters of the interface were experimentally investigated. The obtained values were used to numerically simulate the cohesive behavior of a single crack. These numerical simulations are performed for different lengths and volume fractions of fibers. Results will serve as a basis for selection of suitable fiber type, length and volume fraction to be used in the developed composite.

*Keywords: Lime mortars, Fiber reinforcement, Micromechanical parameters*

## **1. INTRODUCTION**

At the present time a number of restoration works and repairs are carried out on historical monuments. In order to minimize intervention to heritage structures and also for economic reasons it is necessary to correctly identify the causes of the failures and propose arrangements that would resist them. One of many causes of failures can be excessive tensile deformations imposed onto masonry structures. These can result from soil deformation in the foundation, temperature fluctuations or seismicity, whether of natural or artificial origin. Failures in masonry occur mostly in the form of cracks. These cracks then can pave the way for penetration of water and contaminants into the structure, which causes further degradation. One way to alleviate the degradation is to use materials capable of resisting tensile strain while exhibiting narrow cracks, which are less vulnerable to penetration of contaminants. Our intention is to develop mortar with lime matrix reinforced with fibers, which shows pseudo-ductile and strain hardening behavior during tensile deformation and fractures in the form of fine distributed cracks – exhibits so-called multiple cracking. To this end we use the methodology developed for systematic design of brittle-matrix composites reinforced with short fibers. This methodology was successfully used, for example, for design of Engineered Cementitious Composites – ECC [1]. Bridging effect of fibers crossing a crack has a dominant influence on whether the material can exhibit multiple cracking [2]. The goal of this study is to predict of the cohesive relation of a fiber-bridged crack (relation between crack opening displacement and bridging stress) based on micromechanical parameters of fibers and interfaces obtained from realized experiments.

## **2. BEHAVIOR OF A SINGLE FIBER**

Fiber reinforcement in a composite plays an important role during formation and opening of cracks. In this process, crack-bridging fibers are elastically stretched and pulled out from the surrounding matrix.

---

<sup>1</sup> Ing. Přinosil Michal, Czech Technical University in Prague, Faculty of Civil Engineering, Thákurova 7, 166 29, Praha 6, Czech Republic, michal.přinosil@fsv.cvut.cz

<sup>2</sup> Prof. Ing. Kabele Petr, PhD., Czech Technical University in Prague, Faculty of Civil Engineering, Thákurova 7, 166 29, Praha 6, Czech Republic, petr.kabele@fsv.cvut.cz

The whole process can be described by the relationship between force  $P$  on the pulled end of the fiber and the displacement  $u$  at the same point. When a crack forms, force in a bridging fiber, which corresponds to chemical bond  $G_d$  of the fiber with matrix, is activated. With increasing opening of the crack, the fiber debonds from the matrix, which can be viewed as propagation of a tunnel crack along the interface. The force in fiber rises due to activation of frictional stress  $\tau_0$  on the interface, which acts against the fiber slipping direction. The resulting  $P$ - $u$  relation has been derived in ref. [3] as:

$$P_{deb} = \sqrt{\frac{\pi^2 \tau_0 E_f d_f^3}{2} u + \frac{\pi^2 G_d E_f d_f^3}{2}} \quad (1)$$

where  $d_f$  is the fiber diameter,  $E_f$  is Young's modulus of elasticity of the fiber.

The length of the debonded part of the fiber is determined by the balance of forces. The debonding process ends when the debonded length reaches the embedment length  $L_e$ . The displacement of the pulled end of the fiber at this stage is according to ref. [3]:

$$\delta_c = \frac{2\tau_0 L_e^2}{E_f d_f} + \sqrt{\frac{8G_d L_e^2}{E_f d_f}} \quad (2)$$

The first debonding phase is followed by the phase of fiber pull-out. During that, the fiber slips out from the matrix while the contact area with the matrix diminishes. The pull-out phase is described as [3]:

$$P_{pull} = \pi d_f \tau_0 \left( 1 + \frac{\beta(u - \delta_c)}{d_f} \right) (L_e - u + \delta_c) \quad (3)$$

where  $\beta$  is a fiber-matrix interface slip-hardening parameter. The whole  $P$ - $u$  relation is shown in Fig. 1.

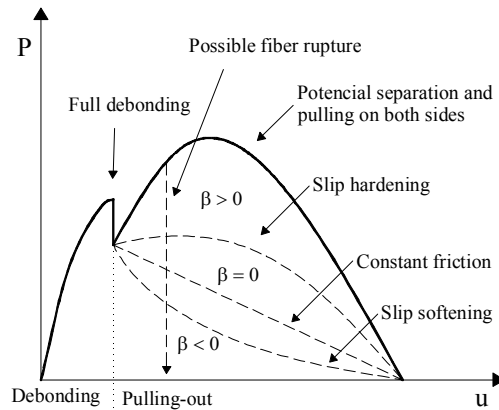


Fig. 1 Single fiber pull-out response

### 3. TESTING OF MATERIAL PARAMETERS

#### 3.1. Selection of materials

At the beginning of the experimental research it was necessary to select suitable components of the sought composite, in particular the fibers. During the selection, natural and synthetic fibers were considered. The main argument for the use of natural fibers is their traditional use in historic mortars [4]. The disadvantages of natural fibers include inherent scatter of their properties and our limited ability to modify these properties. A significant disadvantage of vegetable fibers is their rapid mineralization in alkaline environment of lime mortar [5], which leads to reduction of elasticity and tensile strength and increase in cohesion in contact with surrounding matrix. Therefore, their use was refused. During selection, economical and mechanical criteria were considered and the availability of the fibers on the market was taken into account as well. Eventually, the best match for the given criteria was achieved with fibers from horse (also marked as H), goat (G) and pig (P). From synthetic fibers, polyvinyl-alcohol (PVA – type REC15, made by Kuraray Company) were selected, which have been previously-successfully used in ECC materials.

Considering the general preference to use lime mortars for restoration works, the matrix consisted of hydrated air lime powder, fine quartz sand (maximum particle size 0.3 mm) and water, mixed at volume ratio of approximately 1:2:1.

### 3.2. Testing set-up

Experimental program was designed in order to determine micromechanical parameters of fibers and interfaces between fibers and matrix. The program involved a uniaxial tensile test for obtaining fiber material parameters and the so-called pullout test for obtaining interface parameters. Each group of fibers was represented by 10 specimens for every test, except the PVA group for tensile test. The latter series included only 5 specimens as it was considered that the properties of PVA fibers do not vary too much. Both experiments were performed by means of the MTS Alliance RT/30 machine. The tests were controlled by the crosshead displacement applied at constant rate of 0,3 mm/min and the force, crosshead displacement, and deformation of extensometer (only during the tensile test) were continuously recorded. Furthermore, optical measurement of displacement was performed using high-resolution digital camera with macro lens. Both testing set-ups are shown in Figure 2. Before the uniaxial tests, the diameter of individual fibers  $d_f$  was measured in optical microscope. Fibers were then glued to jigs attached to the loading machine and the free length of the fibers was measured by optical measurement. The free length was typically 5 mm. From the obtained stress-strain diagram Young's modulus of elasticity  $E_f$  and tensile strength  $f_t$  of individual fibers were evaluated.

The specimens for the pullout tests were prepared using the methodology proposed in ref. [6] – see Figure 3. Each tested fiber was first inserted into a blunt medical injection needle, so that the part to be embedded into matrix was protruding out. The fiber was fixed to the needle with soft wax and the length of the protruding part was measured in optical microscope (typically it was 3 mm). The needle was then affixed in the center of a plastic mold, which was subsequently filled with the fresh lime mortar (matrix) so that the end of the needle containing the fiber remained about 5 mm below the mortar surface. By this way it was made sure that the fiber was embedded below the surface layer, which might be possibly weakened by higher porosity or shrinkage micro cracks. All specimens were allowed to harden for 180 days in room conditions. Before testing, the wax fixing fiber inside needle was molten by short heating to 55°C and the needle was carefully extracted, ideally leaving one end of the fiber embedded in the matrix and the other protruding out of the specimen. While this method has previously worked well with PVA fibers in cementitious matrix, in case of the lime matrix many fibers were pulled out of the matrix instead of the needle in this process. This indicates that very low bond acted on the fiber matrix interface – lower than that between the fiber and soft wax. All horse specimens and all except one of the goat, one of the pig specimens showed this behavior. On the other hand, all but four specimens with PVA fibers were extracted successfully.

The successfully prepared specimens were then subjected to the pullout test. The mold with matrix was fixed to the loading frame and the protruding fiber was attached by glue and clip to a jig connected to a load cell. From the measured data, fiber-matrix chemical bond  $G_d$ , frictional bond strength  $\tau_0$  and fiber-matrix interface slip-hardening parameter  $\beta$  were evaluated.

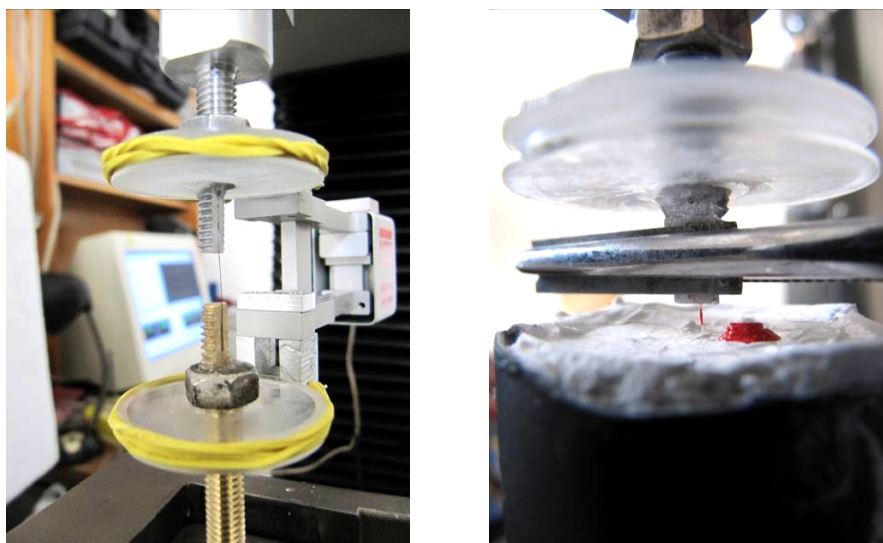


Fig. 2 Testing set-up – uniaxial tensile test (left) and pullout test (right)

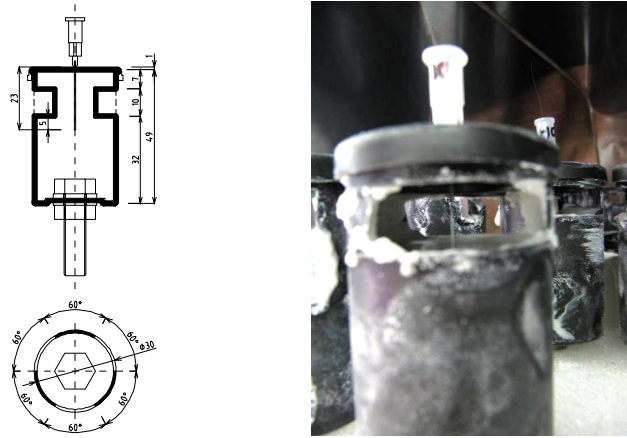


Fig. 3 Specimen for pullout test – drawing (left) and photo (right) [6]

## 4. RESULTS OF THE TESTS

### 4.1. Uniaxial tensile test

Figure 4 shows the stress-strains diagrams for each group of fibers. The graphs show that the behavior of organic fibers is almost bilinear and that these fibers have a high ductility in the tens of percent. Young's modulus of elasticity  $E_f$  was evaluated from the initial linear part. We evaluated tensile strength  $f_t$  of organic fibers as the load level at which the fiber began to distinctively yield. In the case of PVA fibers, which did not exhibit any significant yielding,  $f_t$  corresponds to the load level at which fiber ruptured.

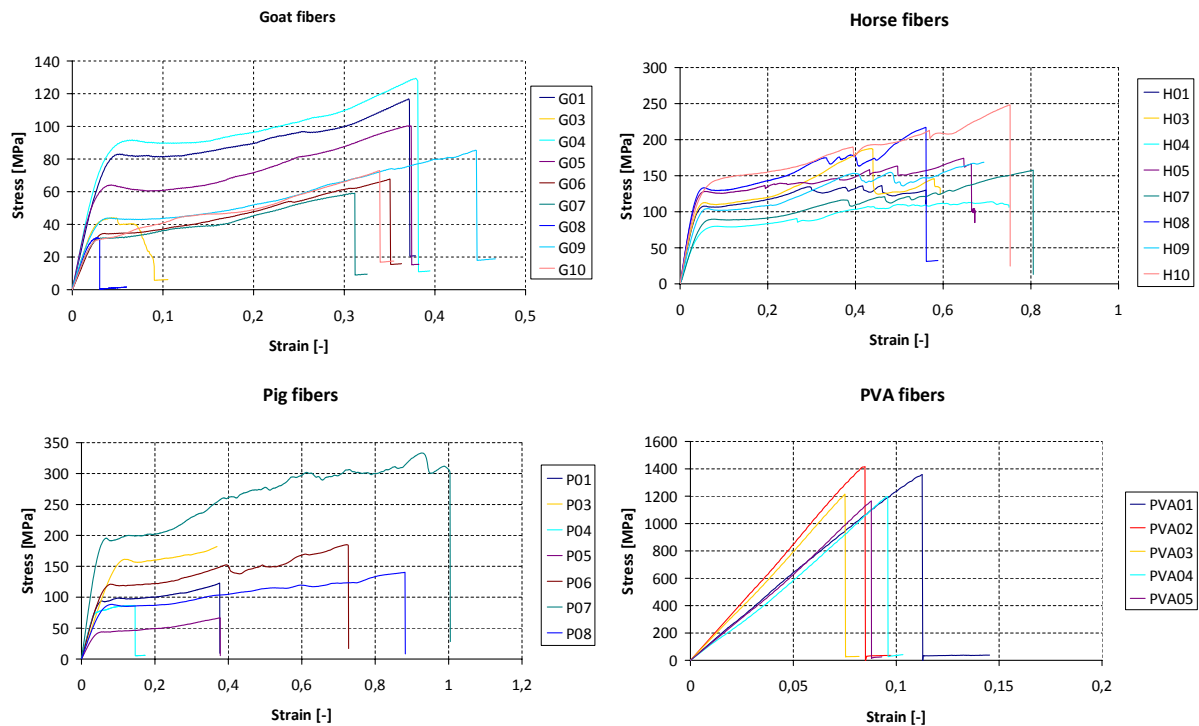


Fig. 4 Stress – strain diagrams from the uniaxial tensile tests for individual groups of fibers

The evaluated micromechanical parameters of fibers are summarized in Table 1.

Table 1 Micromechanical parameters of fibers

	Goat			Horse			Pig			PVA		
	$d_f$	$E_f$	$f_t$	$d_f$	$E_f$	$f_t$	$d_f$	$E_f$	$f_t$	$d_f$	$E_f$	$f_t$
	[ $\mu\text{m}$ ]	[MPa]	[MPa]	[ $\mu\text{m}$ ]	[MPa]	[MPa]	[ $\mu\text{m}$ ]	[MPa]	[MPa]	[ $\mu\text{m}$ ]	[MPa]	[MPa]
MEAN	112,2	2093,5	50,3	140,4	2645,1	109,3	206,0	2203,1	111,0	40,0	13936,8	1269,9
ST.DEV.	5,8	535,2	21,4	25,4	1155,4	18,1	40,6	936,5	47,7	0,0	2029,3	98,1
COV	0,052	0,256	0,426	0,181	0,437	0,166	0,197	0,425	0,429	0,000	0,146	0,077

## 4.2. Pullout test

Figure 5 shows the responses obtained in pullout tests as the relation between force and displacement of crosshead. Individual curves were fitted by Eq. (1) – (3). During the processing, elastic deformation of the free fiber part between the embedment and the fixing jig had to be taken into account (Fig. 2 right). This length could not be directly measured and it was derived from initial slope of the graph. The parameter  $G_d$  was derived from the load level at which debonding of fiber started, which in the graphs corresponded to the first significant reduction of slope (points A in Figure 5). The value of frictional stress  $\tau_0$  was calculated from the load level at the end of the debonding phase (points B in Figure 5). Finally, the parameter  $\beta$  was calculated by using the least-square method to fit the Eq. 3 to the measured data between points C and D in Figure 5.

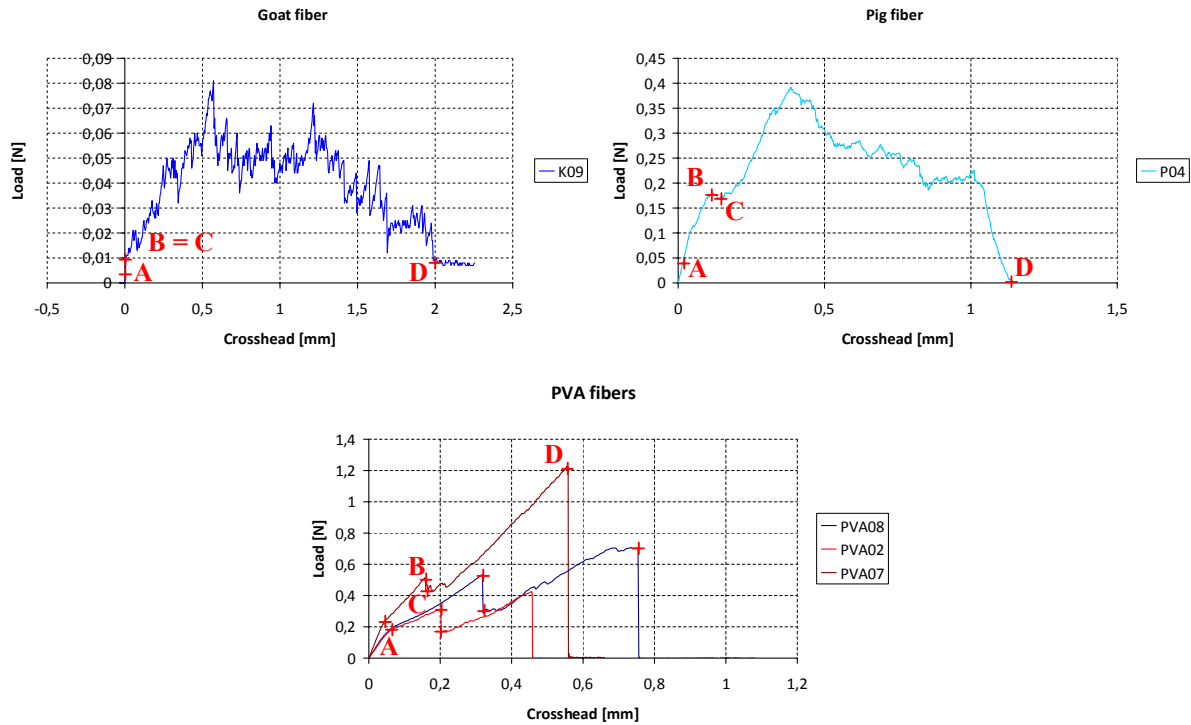


Fig. 5 Force-displacement relations from the pullout tests for individual groups of fibers

Evaluated micromechanical parameters of interface between fibers and lime matrix are summarized in Table 2.

Table 2 Micromechanical parameters of fiber-matrix interface

	Goat			Pig			PVA		
	$\tau_0$ [MPa]	$G_d$ [J/m <sup>2</sup> ]	$\beta$ [-]	$\tau_0$ [MPa]	$G_d$ [J/m <sup>2</sup> ]	$\beta$ [-]	$\tau_0$ [MPa]	$G_d$ [J/m <sup>2</sup> ]	$\beta$ [-]
MEAN	0,015	0,000	1,100	0,220	0,00005	1,100	0,790	0,006	0,367
ST.DEV.	-	-	-	-	-	-	0,269	0,002	0,085
COV	-	-	-	-	-	-	0,340	0,272	0,232

## 5. PREDICTION OF COHESIVE RELATIONS OF FIBER-BRIDGED CRACK

Numerical simulations for each group of fibers were performed to predict the cohesive response of fiber-bridged cracks. By these simulations we predicted the relation between bridging stress  $\sigma_b$  and crack opening displacement  $\delta$  (cohesive relation). The stress  $\sigma_b$  was calculated as the sum of all forces transferred by fibers bridging a crack divided by the crack area  $A_c$ :

$$\sigma_b = \frac{\sum P(\delta)}{A_c} \quad (4)$$

The forces in fibers can be expressed by Eqs. (1) – (3). Furthermore, in these simulations we considered possible fiber rupture, which occurs when the stress in a fiber reaches its tensile strength  $f_t$ . The fiber end displacement  $u$  was related to crack opening displacement  $\delta$  considering that a fiber may debond and pullout on both sides of the crack. Typical examples of the calculated  $\sigma_b$ - $\delta$  relations are illustrated in Figure 6. For the material design purpose, as mentioned in Section 1, we are most interested in the maximum bridging stress  $\sigma_{mb}$  (see Fig. 6 right).

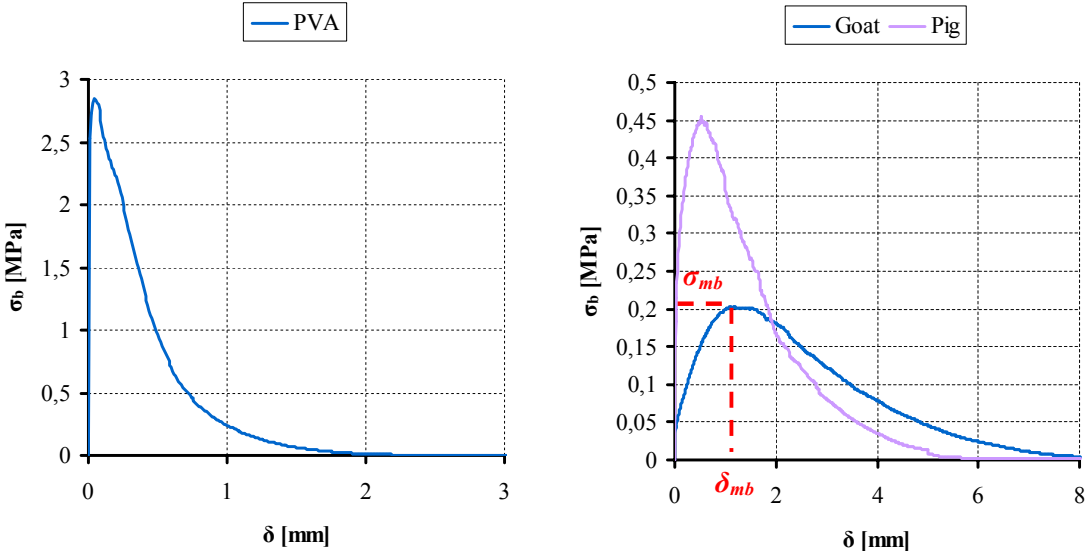


Fig. 6 Typical  $\sigma_b$ - $\delta$  relation for specimen with PVA fibers (left) and goat or pig fibers (right) with  $L_f=20$  mm and  $V_f=0,020$

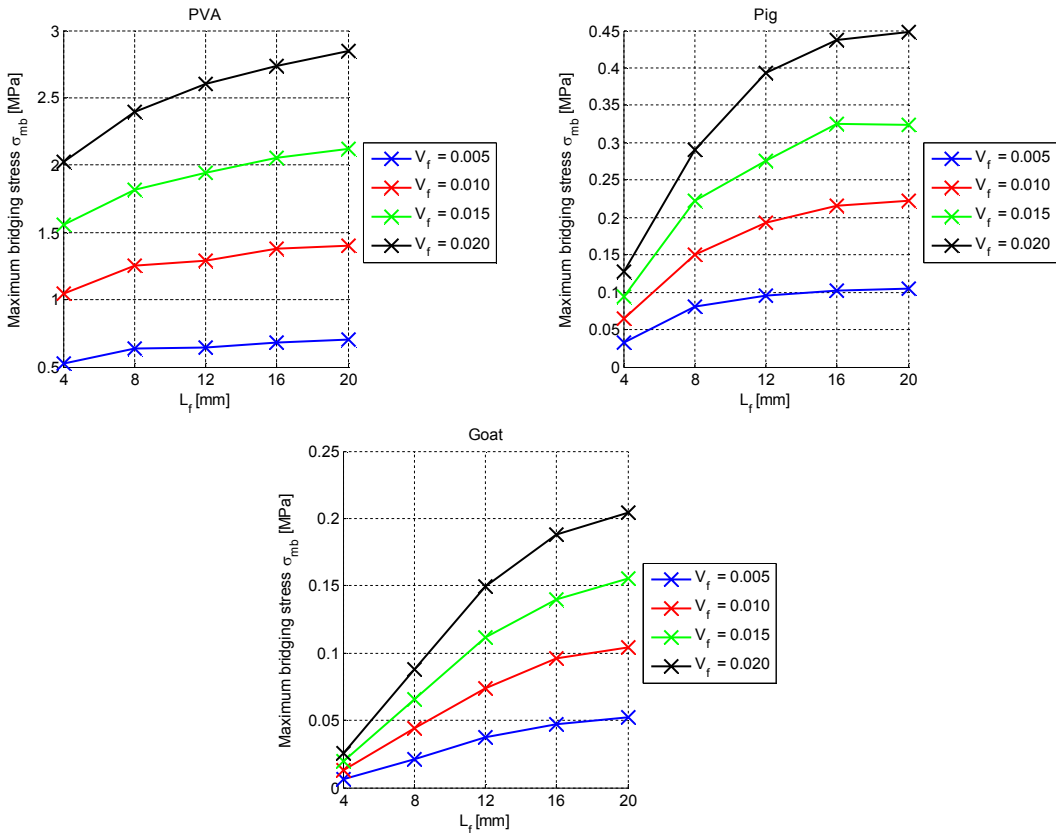


Fig. 7 Maximum bridging stress  $\sigma_{mb}$  for each configuration of parametric study.

The simulation was performed so that, first, fibers of uniform length and diameter were randomly generated in a prismatic volume with the size of  $50 \times 50 \times 250$  mm, which represented a specimen of the composite. The dimensions of the cross-section were chosen so that specimen's size did not

significantly affect the results. The number of fibers was determined by the volume of the specimen, volume of each fiber and by the volume fraction  $V_f$  of fibers in the mixture. Secondly, five crack planes, perpendicular to the specimen axis and with a minimal mutual distance of 20 mm (to avoid interference), were inserted into the specimen. Incrementally increasing crack opening displacement was prescribed to each crack and the corresponding values of bridging stress were calculated using Eq. (4). Results obtained for the five crack planes were then averaged.

A parametric study was performed to determine the effect of fiber length  $L_f$  and fiber volume fraction  $V_f$  on the cohesive response of a fiber-bridged crack. These parameters were chosen since they can be easily varied when designing the reinforced mortar mix. Length of fibers  $L_f$  was considered a) 4 mm b) 8 mm c) 12 mm d) 16 mm e) 20 mm and the volume fraction of fibers  $V_f$  was considered a) 0,5% b) 1% c) 1,5% d) 2%. The upper limit of both the volume fraction and the fiber length were chosen with regard to the workability of the mixture in real conditions. For the remaining micromechanical parameters of fibers and interface, values obtained from experiments discussed in Section 4 were used. The dependence of the calculated maximum bridging stress  $\sigma_{mb}$  on the fiber length  $L_f$  and on the volume fraction  $V_f$  for each group of fibers is shown in Figure 7.

The results show that  $\sigma_{mb}$  is nearly proportional to the volume fraction of fibers  $V_f$  in the mixture. It is also obvious that  $\sigma_{mb}$  increases with the fiber length  $L_f$  but this relation flattens out at certain fiber length. This effect can be attributed to fiber rupture: if the fiber length is too large, fibers tend to rupture before being completely debonded or during the hardening pullout phase. Such fibers then do not contribute to the overall cohesive stress  $\sigma_b$ .

## 6. CONCLUSIONS

One of the criteria for multiple cracking to occur in a brittle-matrix fiber-reinforced composite is that the maximum bridging stress  $\sigma_{mb}$  must be greater than the tensile strength of matrix. Preliminary results for our lime matrix show tensile strength of about 0,35 MPa. As seen in Figure 7, according to the present study, this criterion is not met when workable length and dosage of the organic fibers is used (with the exception of pig fibers added at  $V_f \geq 0.02$  and  $L_f \geq 10$  mm, when the criterion is fulfilled marginally). This can be attributed namely to the low values of chemical bond strength  $G_d$  and the frictional bond  $\tau_0$  that these fibers exhibit. On the other hand, the criterion is safely fulfilled by the synthetic PVA fibers in all examined lengths and volume fractions.

Further work will be thus focused on the use of synthetic fibers. Similar parametric study will be performed also with regards to the crack width, which is determinant for durability. Subsequently optimum fiber length and dosage will be chosen taking into account also workability of the resulting mix. Performance of the resulting composite will be verified by direct tension and bending tests.

## ACKNOWLEDGEMENTS

The presented research has been carried out with financial support of the Czech Ministry of Culture, as part of the project no. DF11P01OVV008.

## REFERENCES

- [1] Li V.C. (2003) On Engineered Cementitious Composites – A review of the material and its applications. *Journal of Advanced Concrete Technology* 1(3): 215-230.
- [2] Marshall D.B., Cox B.N. (1988) A J-integral method for calculating steady-state matrix cracking stresses in composites. *Mechanics of Materials* 7(2): 127-133.
- [3] Li. V.C., Leung C.K.Y. (1992) Steady state and multiple cracking of short random fiber composites. *Journal of Engineering Mechanics* 118(11): 2246-64.
- [4] Moropoulou A., Bakolas A., Bisbikou K. (2000) Investigation of the technology of historic mortars. *Journal of Cultural Heritage* 1: 45-58.
- [5] Drdác M.F., Michoínová D., Procházka P.P. (2002) Maltovinové směsi vyztužené vlákny pro obnovu a záchranu uměleckých památek. *The final report of the research project of the Czech Ministry of Culture no. PK00-P04-OPP15*.
- [6] Novák L. (2010) Mix design and experimental investigation of durability of fiber reinforced cementitious composites. *Ph.D. thesis*, CTU in Prague, Prague.